Theoretical and numerical study of strain rate sensitivity on formability of sheet metal

Cunsheng Zhang, Lionel Leotoing, Dominique Guines, Eric Ragneau

THEORETICAL AND NUMERICAL STUDY OF STRAIN RATE SENSITIVITY ON FORMABILITY OF SHEET METAL

Cunsheng ZHANG*, Lionel LEOTOING, Dominique GUINES, Eric RAGNEAU

INSA, Laboratoire de Génie Civil et Génie Mécanique, Rennes, France

ABSTRACT: In the present work, the formability of an aluminium alloy (AA5083) sheet at elevated temperature ($240°C$ and $300°C$) is investigated by theoretical and numerical approaches, using the Swift hardening law. For the theoretical one, an algorithm based on Newton-Raphson method is developed to calculate the limit strains in the frame of the M-K (Marciniak-Kuczynski) model. Numerically, the M-K model is simulated with the commercially available finite-element code ABAQUS. The comparison between the theoretical and numerical evaluation of FLCs shows a good agreement between two approaches. Finally, the effect of strain rate sensitivity index (m) and forming speed on formability is analyzed. Results reveal that the formability is an increasing function of m while there is no significant influence of forming speed on the sheet formability.

KEYWORDS: Strain rate sensitivity, forming limit diagrams, M-K model

1 INTRODUCTION

The formability evaluation is of considerable practical interest in the sheet metal forming operations, especially with the increasing use of new materials in the automotive and aerospace industry. Forming limit diagrams (FLDs), introduced by Keeler and Backofen [1] in 1963, have been commonly used to evaluate the formability of sheet metals.

The experimental methods for determining FLDs are well established. However, experimental procedures require tremendous amount of effort and special equipments [2]. Therefore, much effort has been made in theoretical prediction of FLDs. Among them, the most frequently used is M-K model, which was developed by Marciniak and Kuczynski in 1967 [3].

Strain rate sensitivity has been experimentally identified as an important factor determining formability of sheet metal and can alter substantially the level and shape of FLDs [4, 5]. However, up to now, relatively little attention has been drawn to the theoretical models taking into account the strain rate sensitivity. Hutchinson et al. [6] predicted the FLDs with Von Mises yield function considering the rate sensitivity. Their work has made important contributions to gaining insight into the roles of constitutive equations and plasticity theories on FLDs. Barata Da Rocha et al. [7] predicted the strain path-dependent FLD by taking into account the rate sensitivity using Hill's theory of plastic anisotropy. Graf and Hosford [8] analyzed the effect of rate sensitivity on the right-hand side of FLD with the Logan and Hosfords anisotropy yield criterion. However, relatively little attention has been paid to the prediction of left-hand side of FLDs because of the complex algorithms and lengthy calculations.

In addition, with the increasing application of computational techniques, numerical predictions of FLDs have become more attractive and the finite element method has been widely adopted in FLDs' determination. Narasimhan and Wagoner [9] have used FEM to predict right-hand side of FLDs in the frame of the M-K model. The influence of material properties, failure criterion, and also defect geometry on the FLD_0 (the limit major strain under the plane strain condition) has been analysed. The shape of FLDs they calculated agreed fairly well with those obtained from the M-K theory. Later, Banabic et al. [10] determined the whole range of FLDs using FE simulation of the M-K model with an inclined groove. For the left-hand side of FLDs, the imperfection orientation was taken according to Hill's zero extension assumption. A good correlation between predicted and experimental results has been obtained for right-side hand of FLDs, while in left area the predicted FLDs underestimate the experimental ones.

Until now, numerical prediction of FLDs taking into account rate sensitivity has never been considered. Hence, the aim of this paper is to evaluate the effect of strain rate sensitivity on formability of an aluminum sheet. Firstly, the constitutive equation parameters in work hardening law are identified for AA5083 at $240°C$ and $300°C$. Then, sheet forma-

*Corresponding author: INSA, Laboratoire de Génie Civil et Génie Mécanique (LGCGM, EA 3913) 20 Av. des Buttes de Coësmes, 35043 Rennes Cedex, France, +33(0)2 23 23 85 22, +33(0)2 23 23 87 26, zhangcs8041@hotmail.com

bility is determined by the theoretical and numerical approaches based on the M-K model with a groove oriented perpendicular to the axis of the largest principal stress. Finally, the effect of strain rate sensitivity and forming speed on formability is analysed by the numerical approach.

2 MATERIAL CONSTITUTIVE LAW

Because of its good formability, AA5083 receives more and more application in automotive and aerospace industry. previous studies have shown a strain rate dependence of the alloy at elevated temperature [11]. Hence, the following multiplicative Swift law has been chosen to describe the viscoplastic behaviour of this AA5083 alloy:

$$\overline{\sigma} = K \cdot (\overline{\varepsilon}_0 + \overline{\varepsilon})^n \cdot \dot{\overline{\varepsilon}}^m \qquad (1)$$

where, $\overline{\varepsilon}$ and $\dot{\overline{\varepsilon}}$ are equivalent plastic strain and equivalent plastic strain rate, respectively. K and $\overline{\varepsilon}_0$ are material parameters, while n and m are the strain hardening and strain rate sensitivity indices.

To characterize the material behaviour of AA5083, tensile tests have been performed on a high-speed servo-hydraulic testing machine (DARTEC, 20KN capacity) at temperatures of $240°C$ and $300°C$ at the constant crosshead speeds of 1.56, 15.6 and 156 mm/s, the true stress-true strain curves are shown in Figure 1 and Figure 2, respectively.

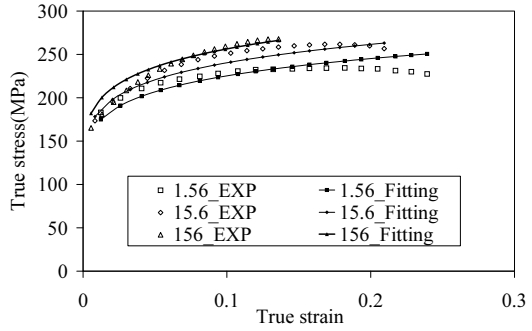

Figure 1: *Experimental and fitting stress-strain curves at $240°C$*

With the least squares optimization, the parameters of above constitutive material model at $240°C$ and $300°C$ have been identified to fit experimental data as shown in Table 1. The corresponding fitting curves are displayed in Figure 1 and Figure 2.

As it can be seen in Table 1, with the increasing temperature, the rate sensitivity index m for AA5083 increases, while the work hardening index n decreases.

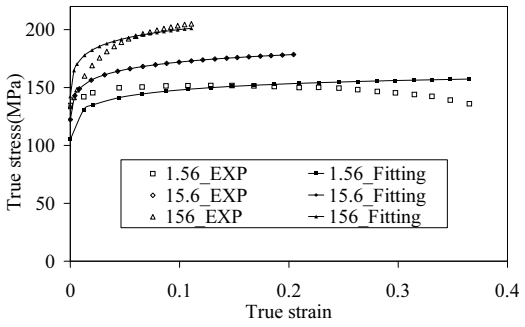

Figure 2: *Experimental and fitting stress-strain curves at $300°C$*

Table 1: *Constitutive model parameters*

$T(°C)$	$K(MPa)$	$\overline{\varepsilon}_0$	n	m
240	328.062	0.00126	0.1275	0.0280
300	207.207	0.00035	0.0614	0.0657

3 THEORETICAL APPROACH

The typical M-K model is shown in Fig. 3. The imperfection is mathematically represented by a long groove which is characterized by an initial imperfection factor

$$f_0 = \frac{e_0^b}{e_0^a} \qquad (2)$$

where e_0^a, e_0^b are the initial sheet thicknesses in zone a and zone b. The indexes a and b are respectively used to designate the outer and the inner regions of the groove.

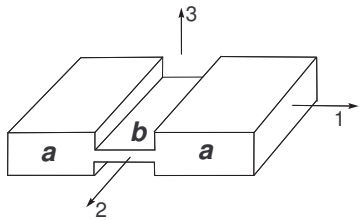

Figure 3: *Representation of the M-K model*

The plastic material behaviour is modelled by the Von Mises yield condition with the plane stress assumption ($\sigma_{13}^k = \sigma_{23}^k = \sigma_{33}^k = 0$):

$$\left(\overline{\sigma}^k\right)^2 = \left(\sigma_{11}^k\right)^2 - \sigma_{11}^k\sigma_{22}^k + \left(\sigma_{22}^k\right)^2 + 3\left(\sigma_{12}^k\right)^2 \qquad (3)$$

where $\overline{\sigma}^k$ is the equivalent stress, σ_{11}^k, σ_{22}^k and σ_{12}^k are stress tensor components ($k = a$ or b)

For the sake of convenience, the following notations are used:

$$\rho^k = \frac{\Delta\varepsilon_{22}^k}{\Delta\varepsilon_{11}^k},\ \Omega^k = \frac{\sigma_{22}^k}{\sigma_{11}^k},\ \varphi^k = \frac{\overline{\sigma}^k}{\sigma_{11}^k},\ \Phi^k = \frac{\Delta\overline{\varepsilon}^k}{\Delta\varepsilon_{11}^k}$$

where Ω^k, φ^k and Φ^k are specific function of ρ^k. For the Von Mises yield function,

$$\begin{aligned} \Omega^k &= \tfrac{2\rho^k+1}{2+\rho^k} \\ \varphi^k &= \sqrt{1-\Omega^k+\left(\Omega^k\right)^2} \\ \Phi^k &= \tfrac{2\varphi^k}{2-\Omega^k} \end{aligned} \tag{4}$$

Combining with the Swift hardening law (1) and the notations (4), the equilibrium equation (i.e. $\sigma_{11}^a e^a = \sigma_{11}^b e^b$) becomes:

$$\frac{(\overline{\varepsilon}_0+\overline{\varepsilon}^a)^n}{\varphi^a}\left(\dot{\overline{\varepsilon}}^a\right)^m = f\frac{(\overline{\varepsilon}_0+\overline{\varepsilon}^b)^n}{\varphi^b}\left(\dot{\overline{\varepsilon}}^b\right)^m \tag{5}$$

where f is the current imperfection factor.
The equivalent strain rate can be similarly expressed by the strain and time increments:

$$\dot{\overline{\varepsilon}}^k = \frac{\Delta\overline{\varepsilon}^k}{\Delta t} \tag{6}$$

where $\Delta\overline{\varepsilon}^k$ is the equivalent plastic strain increment. Δ refers to a quantity corresponding to a small time increment Δt.
Considering the compatibility condition (i.e. $\Delta\varepsilon_{22}^a = \Delta\varepsilon_{22}^b$) and Levy-Mises flow rule, the eq.(5) can be expressed as follows:

$$\begin{aligned} &\tfrac{(\overline{\varepsilon}_0+\overline{\varepsilon}^a)^n}{\varphi^a}\left(\tfrac{2\varphi^a}{2\Omega^a-1}\right)^m \\ &= f\tfrac{(\overline{\varepsilon}_0+\overline{\varepsilon}^b)^n}{\varphi^b}\left(\tfrac{2\varphi^b}{2\Omega^b-1}\right)^m \end{aligned} \tag{7}$$

Clearly observed in eq.(7), with the disappearance of time increment, the level of the strain rate has no effect in the M-K model, therefore, only the rate-sensitivity vis-à-vis the parameter m could be analyzed.
Performing basic mathematical operations and taking into account a small strain increment, the eq.(7) can be written in the form

$$\begin{aligned} &\left(\overline{\varepsilon}_0+\overline{\varepsilon}^a+\Phi^a\Delta\varepsilon_{11}^a\right)^n\tfrac{(\varphi^a)^{m-1}}{(2\Omega^a-1)^m} \\ &= f\left(\overline{\varepsilon}_0+\overline{\varepsilon}^b+\Phi^b\Delta\varepsilon_{11}^b\right)^n\tfrac{\left(\varphi^b\right)^{m-1}}{(2\Omega^b-1)^m} \end{aligned} \tag{8}$$

In zone a, the constant strain path and incremental strain are imposed. For every increment $\Delta\varepsilon_{11}^a$, $\Delta\overline{\varepsilon}^a$ and $\Delta\overline{\varepsilon}^b$ are calculated. The system of the basic equations of the M-K model is solved by the Newton-Raphson method. The computation is stopped until the failure criterion ($\Delta\overline{\varepsilon}^b/\Delta\overline{\varepsilon}^a \geq 7$) is satisfied and the corresponding strains ε_{11}^a and ε_{22}^a at this moment are retained as the limit strains. This point corresponds to a particular strain path defined by the coefficient ρ^a. In order to obtain other points on the FLDs, the computations described above must be performed in a loop controlled by this parameter.
The rheological parameter values at $240°C$ and $300°C$ in Table 1 and the following ones have been used for the computation: e_0^a=1 mm, e_0^b=0.98 mm and $\Delta\varepsilon_{11}^a$=0.0001. The FLCs based on the theoretical approach for AA5083 sheet are displayed in Figure 5.

4 NUMERICAL APPROACH

In this part, the M-K model is simulated with the commercially available finite-element program ABAQUS to numerically analyze the sheet formability. An initial defect in the sheet is characterized by two different zone thicknesses in Figure 4. The sheet is meshed by hexahedral elements. Due to symmetrical boundary conditions, only the half of the entire model is simulated. To compare with the theoretical results, the same constitutive law (1) and the same rheological parameter values in Table 1 as used in theoretical analysis of M-K model are implemented in ABAQUS by using the UHARD user subroutine.
Various strain states can be covered by imposing various displacement ratios at 1 and 2 directions. To determine the limit strains, two different reference elements are required. One of the elements is placed in zone a (Element A), while the other is in zone b (Element B), as shown in Figure 4.

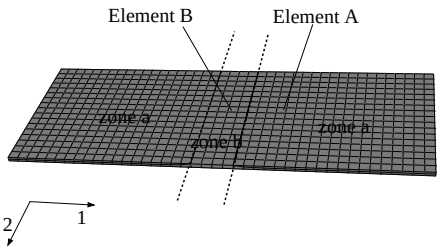

Figure 4: *FEM model in ABAQUS*

When the equivalent plastic strain increment of the Element B exceeds 7 times that in the Element A, the final major and minor strains of Element A are noted as the limit strains in the FLDs. In Figure 5, the limit strains based on FEM are shown for $240°C$ and $300°C$, respectively. For above numerical results, each point corresponds to a certain displacement ratio.
As shown in Figure 5, the FLCs obtained by the two mentioned approaches at 300 $°C$ are slightly higher than those at $240°C$. However, it is worth noticing

that the predictions from the FEM simulations are in good agreement with the values calculated by M-K model. Therefore, it may be concluded that the FEM simulations developed in this work can generate reliable results for the determination of the FLDs.

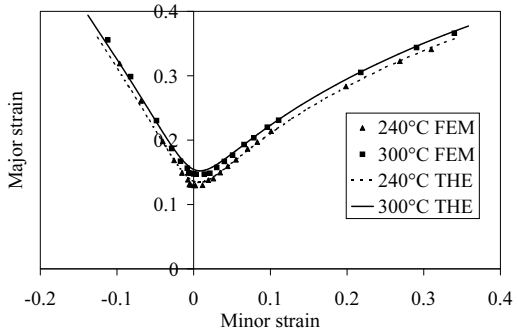

Figure 5: *Theoretical and numerical FLCs of the AA5083 sheet at 240°C and 300°C*

5 EFFECT OF RATE SENSITIVITY AND FORMING SPEED ON FORMABILITY

As was previously stated, the goal of this paper is to evaluate the effect of strain rate sensitivity on formability. But with the theoretical approach, one can not investigate the effect of strain rate on formability. A better way to evaluate this effect is to simulate the necking process by the numerical approach.

5.1 INFLUENCE OF STRAIN RATE SENSITIVITY INDEX ON FLDS

In order to analyze the effect of strain rate sensitivity index m on formability, the rheological parameters under quasi-static condition (i.e. m=0) at 240°C and 300°C are implanted into ABAQUS in order to compare with the above results considering the strain rate sensitivity.

As shown in Figure 6, the influence of strain rate sensitivity index (m) on FLDs can be clearly observed: a high m value produces a high level of the FLDs. For example, in comparison with m=0, there is approximately an increase of 86% for FLD_0 at 240°C, while at 300°C, this value reaches 458%.

As mentioned in Section 4, the FLC at 300°C is slightly higher than that at 240°C. However, the FLCs determined under quasi-static condition show a contrary tendency that the formability is greatly improved with decreasing temperature, i.e. with the increasing value of n. Compared to the formability at 300 °C, there is a 164% increase of FLD_0 at 240°C under quasi-static condition. Now, it is easy to conclude that both strain hardening and strain rate sensitivity indices could enhance the sheet formability by delaying the onset of localized necking. Therefore, to more accurately evaluate a sheet formability, one should take into account its both work hardening and strain rate sensitivity.

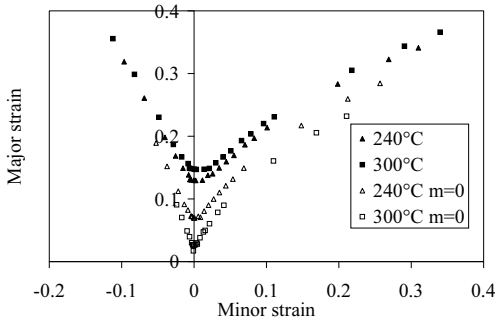

Figure 6: *Effect of rate sensitivity index m on formability*

5.2 INFLUENCE OF FORMING SPEED ON FLDS

To investigate the influence of forming velocity, the FEM condition includes varying forming times (This leads to variation of strain rate). Three scales of forming velocity (represented by the ratio of displacement in the direction-1 and forming times) are chosen: 0.1 mm/s, 2 mm/s and 1200 mm/s. The rheological parameters at 300 °C in Table 1 have been used in the simulation.

Figure 7 shows the effect of forming velocity on the FLDs. At forming speed from 0.1 mm/s to 1200 mm/s, the strain rates from $10^{-2}s^{-1}$ to $10^{2}s^{-1}$ are achieved, but the FLCs do hardly change, so it is concluded that forming velocity has little influence on material formability for the mentioned constitutive law. This conclusion coincides with the fact that the effect of strain rate on formability disappears in M-K model.

6 CONCLUSIONS

In this work, the formability of AA5083 sheet has been investigated by theoretical and numerical approach based on M-K model. Then by numerical approach, the effect of strain rate sensitivity coefficient m and forming speed on formability has been studied. After carrying out the FEM simulation, the following conclusions have been reached:

1 The FEM simulations based on M-K model can generate reliable results for the determination of the FLDs.

2 The formability is found to be significantly sensi-

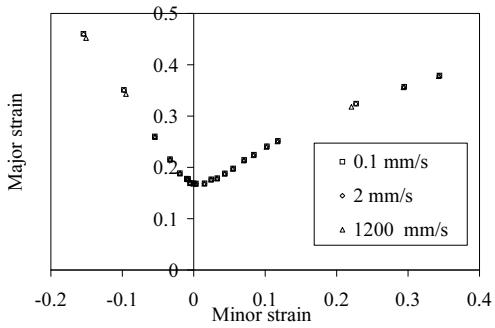

Figure 7: *Effect of forming speed on formability*

tive to the strain rate sensitivity index m.

3 The numerical result shows that the forming speed has little influence on the material formability. It is contrary to what strain rate influences the material formability in the literature [12]. One reason to explain this phenomenon may be that a simplistic hardening law has been used in the above analysis. In the theoretical approach, it also leads to an independence of formability on strain rate. Therefore, a more complex constitutive laws, such as Johnson-Cook or Cowper-Symond law, should be considered. In addition, to validate the numerical result, experimental investigations of strain rate effect on sheet formability are in progress.

REFERENCES

[1] S.P. Keeler and W.A. Backofen. Plastic instability and fracture in sheets stretched over rigid punches. *Transactions of The ASM*, 56: 25–48, 1963.

[2] F. Ozturk and D. Lee. Experimental and numerical analysis of out-of-plane formability test. *Journal of Materials Processing Technology*, 170:247–253, 2005.

[3] Z. Marciniak and K. Kuczynski. Limit strains in the processes stretch-forming sheet metal. *International Journal of Mechanical Sciences*, 9:609–620, 1967.

[4] J.H. Percy. The effect of strain rate on the fld for sheet metal. *Annals of the CIRP*, 29: 151–152, 1980.

[5] P. Broomhead and R.J. Grieve. The effect of strain rate on the strain to fracture of a sheet steel under biaxial tensile stress conditions. *Journal of Engineering Materials and Technology*, 104:102–106, 1982.

[6] J.W. Hutchinson, K.W. Neale, and A. Needleman. *Mechanics of Sheet Metal Forming*, pages 269–285. New York/London, Plenum Press, 1978.

[7] A. Barata da Rocha, F. Barlat, and J.M. Jalinier. Prediction of the forming limit diagrams of anisotropic sheets in linear and non-linear loading. *Materials Science and Engineering*, 68:151–164, 1984-1985.

[8] A. Graf and W. F. Hosford. Calculations of forming limit diagrams. *Metallurgical Transactions A*, 21A:87–93, 1990.

[9] K. Narasimhan and R.H. Wagoner. Finite element modeling simulation of in-plane forming limit diagrams of sheets containing finite defects. *Metallurgical and Materials Transactions A*, 22A:2655–2665, 1990.

[10] D. Banabic, O. Cazacu, L. Paraianu, and P. Jurco. Recent developments in the formability of aluminum alloys. In *Proceedings of the 6th International Conference and Workshop on Numerical Simulation of 3D Sheet Metal Forming Process*, volume 778, pages 466–471, 2005.

[11] S. Diot, D. Guines, A. Gavrus, and E. Ragneau. Forming process of a 5083 aluminium alloy. constitutive model covering a large range of temperature. *International Journal of Forming Processes*, 9:167–188, 2006.

[12] D. Banabic, H.J. Bunge, K. Phlandt, and A.E. Tekkaya. *Formability of metallic material (plastic anisotropy, formability testing, Forming limits)*. Springer-Berlin, Heidelberg, 2000.